

# On the transition between different initiation structures of wedge-induced oblique detonations

Yining Zhang<sup>1</sup>

*Beijing Power Machinery Research Institute, Beijing, 100074, China*

Pengfei Yang<sup>2</sup> and Honghui Teng<sup>3</sup>

*School of Aerospace Engineering, Beijing Institute of Technology, Beijing 100081, China*

*Institute of Mechanics, Chinese Academy of Sciences, Beijing, 100190, China*

Hoi Dick Ng<sup>4</sup>

*Department of Mechanical, Industrial and Aerospace Engineering, Concordia University, Montreal, QC, H3G 1M8, Canada*

and

Chihyung Wen<sup>5</sup>

*Department of Mechanical Engineering, The Hong Kong Polytechnic University, Kowloon, Hong Kong*

Oblique detonation waves (ODW) have been widely studied due to their application potential for air-breathing hypersonic propulsion. Moreover, various formation structures of wedge-induced oblique detonation waves have been revealed in recent numerical investigations. Given the inflow conditions, the wave configuration is dependent on the wedge angle. Hence, any wedge angle change will induce a transient ODW evolution to transition from one configuration to another. In this study, the transient development created by instantaneously changing the wedge angle is investigated numerically, based on the unsteady two-dimensional Euler equations and one-step irreversible Arrhenius chemical kinetics. The evolution caused by the abrupt wedge angle change from one smooth initiation structure to another, both with a curved oblique shock/detonation surface at high Mach number regime is investigated. Two processes are analyzed, the first consists of the downstream transition of the ODW initiation region the by decreasing the angle, and the second is the upstream transition by increasing the angle. In the downstream transition, the overall structure moves globally and re-adjusts continuously, generating an intermediate kink-like initiation structure. In the upstream transition, a localized reaction region forms and induces a more complex process, mainly derived from the different responding speeds of the oblique shock and detonation waves. To avoid the generation of the new localized explosion region which causes an abrupt change in the initiation position and potentially affects the ODWE's stability and performance, it is suggested to vary the wedge angle in incremental steps within a certain time interval.

---

<sup>1</sup> Director and research fellow, State Key Laboratory of Laser Propulsion & Application, Post Box 7208, Beijing.

<sup>2</sup> Graduated student, State Key Laboratory of High Temperature Gas Dynamics, No. 15 Beisihuanxi Road, Beijing.

<sup>3</sup> Professor, Department of Mechanics, No. 5, Zhongguancun south street, Beijing.

<sup>4</sup> Professor, Department of Mechanical, Industrial and Aerospace Engineering, Concordia University, 1515 St.-Catherine St. W., Montreal, QC, Canada, and AIAA senior member.

<sup>5</sup> Professor, Department of Mechanical Engineering, The Hong Kong Polytechnic University, Kowloon, Hong Kong and AIAA associate fellow.

## Nomenclature

$e$	=	total energy
$E_a$	=	activation energy
$k$	=	pre-exponential factor
$L_{1/2}$	=	half reaction zone length
$M_0$	=	flight Mach number
$M_1$	=	pre-detonation inflow Mach number
$p$	=	pressure
$q$	=	heat release of chemical reaction
$R$	=	universal gas constant
$t$	=	time
$T$	=	temperature
$T_0$	=	premixed mixture temperature
$u$	=	velocity in the $x$ - direction
$v$	=	velocity in the $y$ - direction
$\theta$	=	wedge angle
$\gamma$	=	ratio of specific heats
$\rho$	=	density
$\lambda$	=	chemical reaction progress index
$\dot{\omega}$	=	chemical reaction rate

## I. Introduction

FOR a supersonic combustible gas flow past a wedge, depending on the incoming flow condition and the wedge angle, an oblique shock wave (OSW) is attached to the wedge and may trigger the formation of an oblique detonation wave (ODW). The idea of harnessing a standing ODW for hypersonic air-breathing propulsion systems has long been considered and is still under investigation [1–4]. While many theoretical investigations have provided the basic foundation for steady ODWs [5–8], the current research on ODW phenomenon has been towards attaining a better fundamental understanding of its transient formation structure and stability.

Over the past decades, many investigations have been performed which reveal different ODW formation structures. The classical structure of an oblique detonation wave stabilized over a wedge was revealed in the pioneering work of Li et al. [9, 10] by means of numerical simulations and later confirmed experimentally by Viguier et al. [11]. This classical structure is composed of a non-reactive oblique shock, a set of deflagration waves, and the oblique detonation surface, all united on a multi-wave point. The sketch of this structure is illustrated in Fig. 1a, which is referred to as the abrupt transition from OSW to ODW. A different type of formation structure has also been described in Fig. 1b, demonstrating that the transition may occur smoothly from a curved shock [12–14], rather than an abrupt transition through a multi-wave point. The smooth transition usually appears in the cases of high Mach number  $M_I$  and low activation energy  $E_a$ , without cellular structures near the initiation region. Recent studies also reveal more complex ODW formation structures of different wave configurations, with the induction region observed to be ended by an internal Chapman-Jouguet (CJ) detonation wave rather than a set of deflagration waves at low inflow Mach number condition [15–20]. With regards to the established oblique detonation waves, a number of numerical investigations have demonstrated that the ODW is inherently unstable with fine scale instability features on the oblique detonation surfaces similar to the unstable frontal structure of normal cellular detonations [13,21–26].

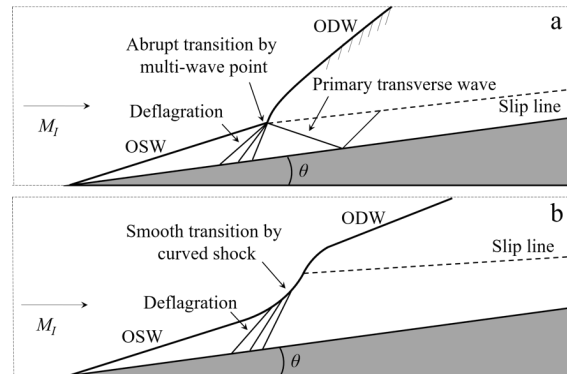


**Fig. 1 Sketch of ODW structures, abrupt transition (a) and smooth transition (b).**

For ODW applications in propulsion systems, it is vital to assess the wave structure dynamics as well as its static configuration. Aforementioned studies [12–20] assume the inflow is well-premixed and uniform, which is seldomly available in practical situations. Therefore, a number of recent studies have been carried out concerning the effect of mixture inhomogeneity of the premixed combustible gas flow on the ODW formation due to incomplete mixing [9, 27–32]. These studies introduced large disturbances composed of a region with radical species or a spatial variation in the equivalence ratio of the flow. The ODW is generally found to be distorted by these disturbances, and in some

cases the formation is replaced by a more complicated structure. However, the effects of nonstationary inflow are not studied so far to the authors' knowledge.

The present numerical study addresses the transitions between different ODW formation structures, which can be viewed as the simplest situation of the nonstationary inflow. It is often impossible to maintain the inflow conditions constant in practical engines, which may induce different ODWs, and some controlling parameters needs to be adjusted accordingly. Apart from the chemical control by changing the amount of fuel injection to vary the energetics of the combustible, a mechanical way to adjust the ODW structure in response to any incoming flow perturbation is by varying the wedge angle. As a first step to describe ODW engine performance in relation to wedge angle variation, this work aims to investigate how one ODW formation structure evolves into another and the related flow field dynamics. Two typical smooth ODW formation structures are first introduced, whose initiation positions are controlled by the wedge angle with the same incident or inflow Mach number. The dynamic transition process is induced by an instantaneous wedge angle variation, and two kinds of processes are observed and analyzed.

## II. Physical model and computational method

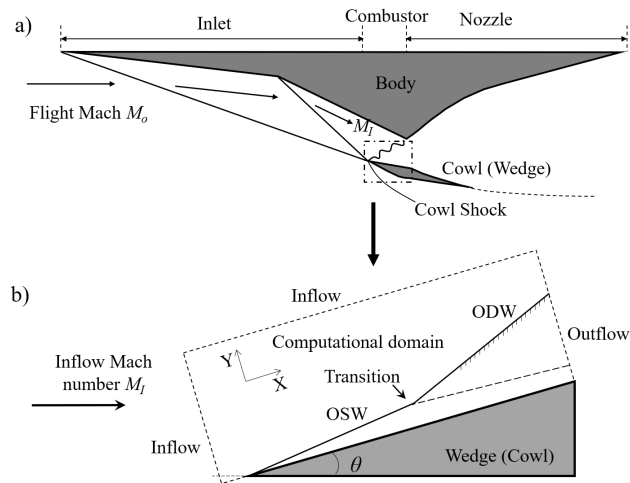


**Fig. 2 Sketch of an oblique detonation engine and simulation settings.**

A schematic of an ODW engine [33] and the wedge-induced oblique detonation is shown in Fig. 2. The combustible inflow reflects on the two-dimensional wedge, and high temperature may trigger exothermic chemical reactions and lead to the onset of an oblique detonation wave. As shown in Fig. 2a, the current study focuses only on the cowl region enclosed by the dashed lines with variable wedge angle. The inflow Mach number  $M_I$  is prescribed

for the present simulation, i.e., the effect of impinging oblique shocks are not investigated. For the present numerical study, the computational domain bounded by the dashed zone is also shown in Fig. 2b, whose coordinates are aligned with the wedge surface. Previous numerical studies [10, 12] indicate that the viscosity and boundary layer have little effects on this structure except changing the boundary layer thickness slightly. Hence, following most of the previous numerical studies [13-26], the present study is also based on the inviscid assumption. The non-dimensional governing equations with a single-step, irreversible chemical reaction are of the form:

$$\frac{\partial U}{\partial t} + \frac{\partial E}{\partial x} + \frac{\partial F}{\partial y} + S = 0 \quad (1)$$

$$U = \begin{bmatrix} \rho \\ \rho u \\ \rho v \\ \rho e \\ \rho \lambda \end{bmatrix}, E = \begin{bmatrix} \rho u \\ \rho u^2 + p \\ \rho uv \\ \rho u(e + p) \\ \rho u \lambda \end{bmatrix}, F = \begin{bmatrix} \rho v \\ \rho uv \\ \rho v^2 + p \\ \rho v(e + p) \\ \rho v \lambda \end{bmatrix}, S = \begin{bmatrix} 0 \\ 0 \\ 0 \\ 0 \\ \dot{\omega} \end{bmatrix} \quad (2)$$

with

$$e = \frac{p}{(\gamma - 1)\rho} + \frac{1}{2}(u^2 + v^2) - \lambda Q \quad (3)$$

$$p = \rho T \quad (4)$$

$$\omega = -k\rho(1 - \lambda) \exp(-E_a/T) \quad (5)$$

All the flow variables have been made dimensionless by reference to the uniform unburned state ahead of the detonation front,

$$\rho = \frac{\tilde{\rho}}{\tilde{\rho}_0}, p = \frac{\tilde{p}}{\tilde{p}_0}, T = \frac{\tilde{T}}{\tilde{T}_0}, u = \frac{\tilde{u}}{\sqrt{\tilde{R}\tilde{T}_0}}, Q = \frac{\tilde{Q}}{\tilde{R}\tilde{T}_0}, E_a = \frac{\tilde{E}_a}{\tilde{R}\tilde{T}_0} \quad (6)$$

For the chemical reaction,  $\lambda$  is the reaction progress variable which varies between 0 (for unburned reactant) and 1 (for product). The reaction is controlled by the activation energy  $E_a$  and the pre-exponential factor  $k$ , and the latter is chosen to define the spatial and temporal scales. The governing equations are discretized on Cartesian uniform grids and solved with the MUSCL-Hancock scheme with Strang's splitting. The MUSCL-Hancock scheme is formally a second-order extension to the Godunov's first order upwind method by constructing the Riemann problem on the inter-cell boundary [34]. The scheme is made total variation diminishing (TVD) with the use of slope limiter MINBEE, and the HLLC approximate solver is used for the Riemann problem.

The inflow is assumed to be calorically perfect and well premixed, so the chemical reaction can be represented by one-step irreversible heat release model with  $\gamma$ ,  $E_a$  and  $Q$ . This chemical reaction model is the simplest model and

widely used in predicting certain detonation behavior, such as one-dimensional detonation instability [35, 36], cellular structures of the normal detonation [37, 38] and instability of oblique detonations [25, 26]. It should be noted that the single-step chemical kinetics has its limitation and is known to have an impact in predicting certain detonation behavior, i.e. pathological detonations [39, 40]. Considering the heat release process of this study is oblique-shock induced combustion and the success in predicting salient ODW behaviors from previous studies [13-17, 21-26], the one-step irreversible heat release chemical model is adopted. The present simulation uses the dimensionless parameters  $E_a = 20$ ,  $Q = 50$  and  $\gamma = 1.2$ . These are traditionally used in numerical simulations as canonical values to investigate detonation wave phenomena in general, only  $E_a$  is decreased to include the effects of the high altitude. Assuming the calorically perfect inflow is the basis for the use of the one-step irreversible heat release model, which neglects the real gas effects and the complexity of chemistry, usually concerning tens of species and hundreds of elemental reactions. Nevertheless, this simple model is sufficient because this study mainly focuses on the shock-induced combustion qualitatively as well as the overall ODW initiation dynamics, and the present computational study benefits from its simplicity.

Inflow conditions are fixed at the free-stream values in both the left and upper boundaries of the domain. Outflow conditions extrapolated from the interior are implemented on the right and lower boundaries before the wedge. Slip boundary conditions are used on the wedge surface, which starts from  $x = 0.5$  on the lower boundary. Initially the whole flow field has uniform density, pressure, and velocities, which are calculated according to  $M_I$  and  $\theta$ . The pre-exponential factor  $k$  is determined to scale the half-reaction length  $L_{1/2}$  to unity, and  $M_I$  is fixed to be 12 in all simulations.

In this investigation, a stationary formation structure corresponding to a given  $M_I$  and  $\theta$  is first simulated. This stationary structure is then used as the initial condition in the successive transient simulation, with the same  $M_I$  but different  $\theta$ . It is worth noting that, with this computational approach, the finite time required for the wedge angle change is not exactly considered. However, the mechanical adjustment may occur much faster than the flow field evolution. For example, an angle adjustment of  $6^\circ$  has the characteristic time on the scale of  $10^{-5}$  s by using the industrial motor with  $10^5$  rpm (round per minute). On the other hand, the heat release process in the normal detonation usually has a characteristic length on the scale of  $10^{-2}$  m, but because of the low density at high altitude and the long inert oblique shock shown in the later figures, the characteristic length of this study is easy to reach the scale of  $10^{-1}$  m. Considering the velocity  $10^3$  m/s, the flow characteristic time is  $10^{-4}$  s, about one-order higher than that of angle

variation. Hence, neglecting the finite time required for the wedge angle change is a reasonable assumption, although some physical details during the finite intermediate time of wedge angle movement may not be fully captured, e.g., expansion growth and pressure waves generated through the finite time wedge angle variation. The time instant  $t = 0$  thus denotes the start of the new transient simulation in this study to investigate the dynamics of the transition process between structures induced by different instantaneous changes of wedge angle.

### **III. Numerical results and discussion**

#### **A. ODW structures and resolution study**

From the viewpoint of the OSW to ODW transition, there are two types of ODW structures. The abrupt transition is featured by the multi-wave point, and the smooth one by the curved shock, as shown in Fig. 1. Moreover, previous studies [30, 41] demonstrate that the smooth transition with a curved shock appears when considering the inflow conditions of the oblique detonation engines. Results with  $\theta = 18^\circ$  and  $24^\circ$  are shown in Fig. 3, illustrating two structures with the smooth transition as expected. The OSW–ODW transition can be viewed as the ODW initiation, and the initiation position is found to depend on the wedge angle significantly. With lower  $\theta$ , the ODW initiation occurs further downstream, and vice versa. These ODW structures and their dependence on  $\theta$  agree with previous studies [12-24].

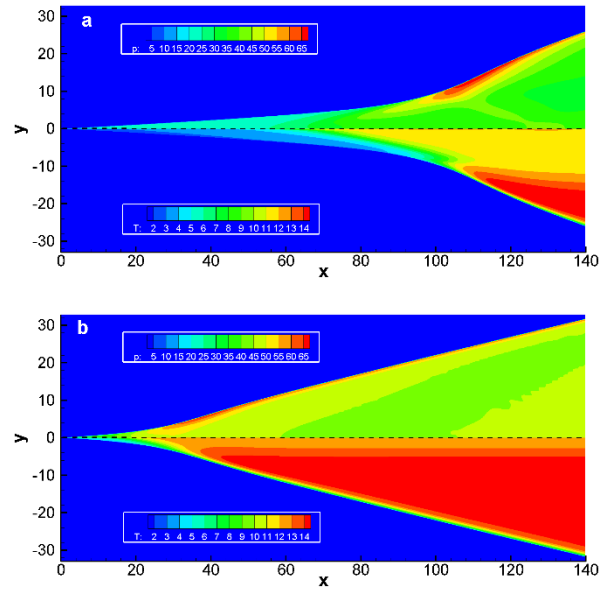


Fig. 3 Pressure (upper) and temperature (lower) fields of the ODW structures with  $\theta = 18^\circ$  (a) and  $24^\circ$  (b).

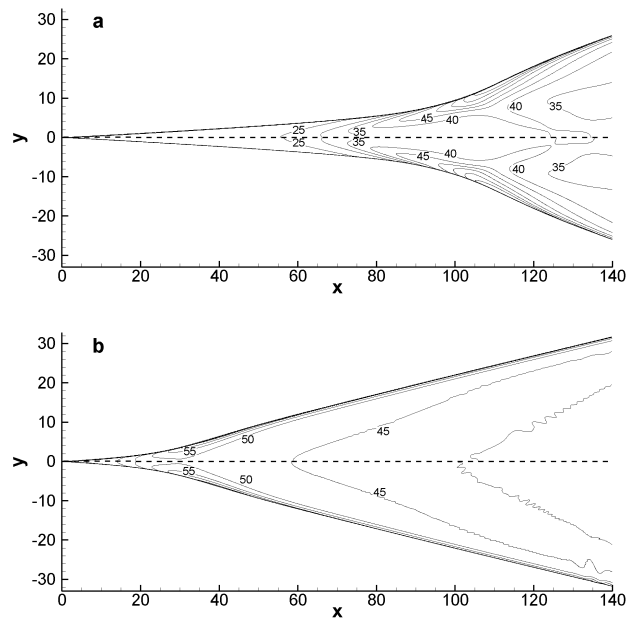
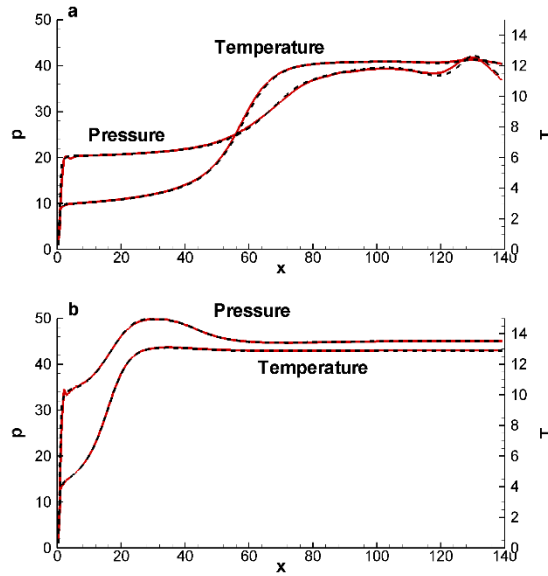


Fig. 4 ODW structure by pressure flow field with  $\theta = 18^\circ$  (a) and  $24^\circ$  (b), in each frame 16 (upper) and 32 (lower) grids per  $L/2$ .





**Fig. 5 Pressure and temperature plots along the wedge with  $\theta = 18^\circ$  (a) and  $24^\circ$  (b), in each frame 16 (red solid lines) and 32 (black dashed lines) grids per  $L_{1/2}$ .**

Detonation simulations with different grid sizes are carried out using the same initial and mixture conditions in order to verify the effect of numerical grid resolution. The pressure contours with 16 and 32 grid points per  $L_{1/2}$  of a corresponding CJ detonation are shown in Fig. 4. Only a slight difference of certain pressure contour position is observed, and the flow fields are almost the same for both cases. For better illustration, the corresponding pressure and temperature plots of the two wedge angle cases along the wedge are also given in Fig. 5, showing good agreement between the results from the two grid resolutions. Furthermore, by examining the reaction progress variable  $\lambda$ , it is found that a numerical resolution of 16 points per  $L_{1/2}$  of a CJ detonation equivalently provides about 20 points per  $L_{1/2}$  along the  $x$ - direction for the  $\theta = 18^\circ$  case, and 40 points per  $L_{1/2}$  for the  $\theta = 24^\circ$  case. This can be thought of as the true resolution to capture the oblique shock and heat release coupling, which is already higher than the resolution used in our previous studies [25,26,41]. This investigation uses the relatively low  $E_a = 20$  for considering the inflow conditions of the oblique detonation engines roughly. This makes the change of the reaction progress variable  $\lambda$  relatively less temperature-sensitive, so that cellular structures are absent in the limited computational domain. Previous numerical resolution study [42] has demonstrated that the regular detonation with low activation energy is much easier to converge with less grids per half reaction zone. Consequently, a smoother reaction profile can be

generated with less numerical grid resolution and the resolution of 16 grid points per  $L_{1/2}$  of a CJ detonation is considered acceptable to simulate the ODW structure with the given parameters in the subsequent simulations.

### **B. Downstream transition induced by decreasing $\theta$**

By decreasing  $\theta$  from  $24^\circ$  to  $18^\circ$ , the ODW structure changes and the initiation position moves downstream. Theoretically, this will induce the oblique shock angle adjusting slightly from  $3.6^\circ$  to  $3.1^\circ$ , but the post-shock temperature changes from 4.0 to 2.8. The latter decreases the chemical reaction rate causing the initiation position to move downstream. Numerical results of the dynamic transition process are shown in Fig. 6. In the initial stage, it is easy to observe the shift of the initiation position toward downstream. As shown in Fig. 6b, a kink-like initiation structure is formed initially and a local high-density region appears below the OSW. The reaction progress with  $\lambda = 0.5$ , denoted by the black line, has a spike penetrating into the combustion product, as shown in Fig. 6c. The oblique shock extends further downstream, generating the high-density region behind the curved shock (Fig. 6d). The structure shown in Fig. 6f approaches to the final stationary configuration as given in Fig. 3a, except the presence of a transverse wave moving downstream along the oblique detonation surface. Generally, the new structure evolves continuously around the original upstream initiation point and then spreads downstream. This flow evolution can be viewed as a global downstream movement of the initiation region. Nevertheless, during the ODW structure evolution, the adjustment to the change of wedge angle is not a simple shift of the complete structure downstream. This leads to a dynamic transition and gives rise to the observed intermediate structure.

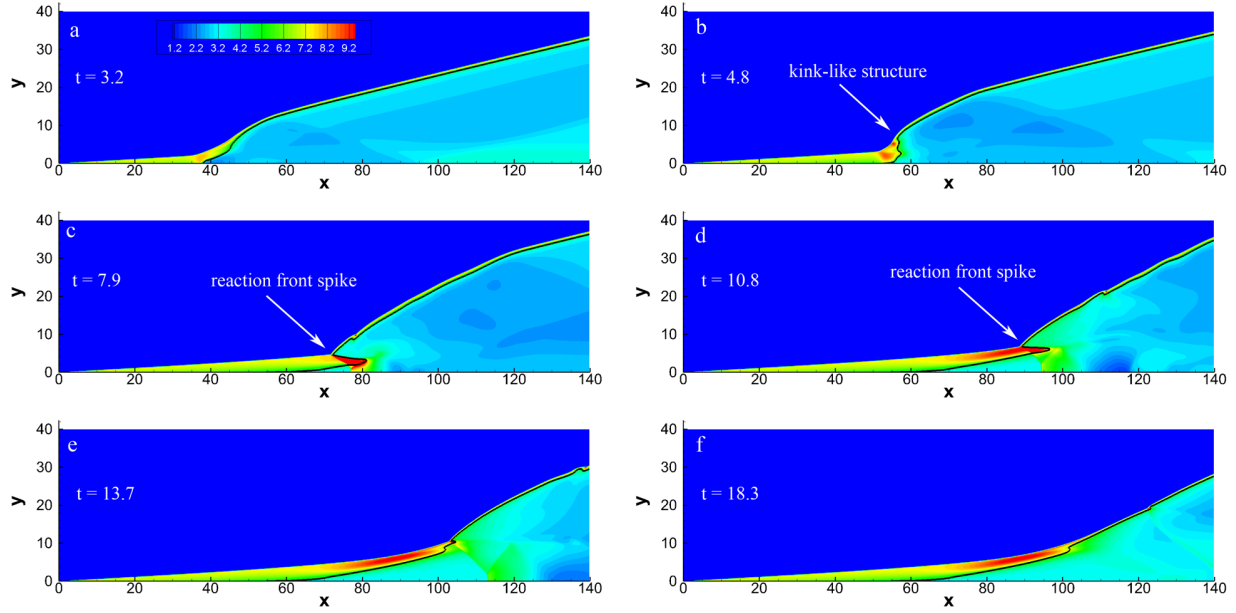


**Fig. 6** Evolution of the density field (with black line denoting  $\lambda = 0.5$ ) when  $\theta$  changes from  $24^\circ$  to  $18^\circ$ .

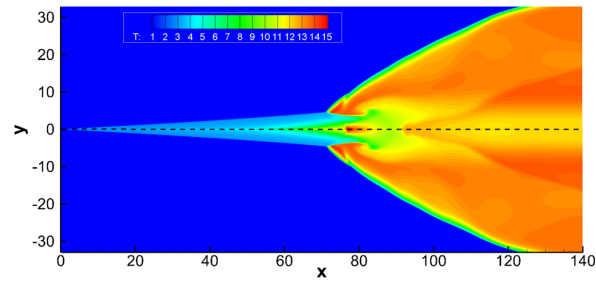


**Fig. 7** Temperature fields when  $\theta$  changes from  $24^\circ$  to  $18^\circ$ , in each frame 16 (upper) and 32 (lower) grids per  $L_{1/2}$ .

Since this study focuses mainly on the dynamic transition of different ODW structures, another resolution study of the transient process is performed, as shown in Fig. 7. The temperature fields show clearly the oblique shock and detonation fronts, the multi-wave complex near the transition, and the wave in the combustion product. It is observed that the flow fields are almost the same for both cases, demonstrating the resolution used here is acceptable to simulate the ODW structure with the given parameters in the subsequent simulations.

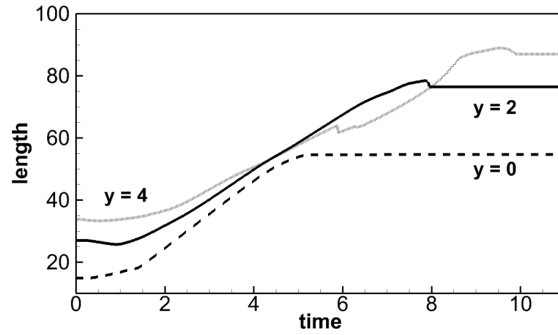


**Fig. 8 Initiation length along  $y = 0, 2$  and  $4$  when  $\theta$  changes from  $24^\circ$  to  $18^\circ$ .**

To elucidate the temporal features of the observed structure evolution, the initiation length along different lines parallel with the  $x$ -axis, defined from the oblique shock ( $\lambda = 0.0$ ) to the half reaction surface ( $\lambda = 0.5$ ), are plotted in Fig. 8. The relaxation of the ignition region takes about non-dimensional time  $t = 5.0$ , as shown by the curve along  $y = 0$ , while the evolution of the whole flow field takes  $t > 15.0$ . The initiation length along  $y = 0$ , which corresponds the wedge surface shown by dashed curve, is found to converge quickly: initially it moves downstream slowly but an obvious acceleration can be observed after  $t = 1.5$ ; before it reaches the steady position around  $t = 5.0$ , a gradual deceleration stage can be observed. Nevertheless, the length variation along  $y = 2$  and  $4$  are found to be more complex where different waves interact. For both curves, the length at the initial stage before  $t = 1.0$  decreases slightly. Subsequently, the length along  $y = 2$  increases faster than that along  $y = 4$ , so the two curves intersect with each other. This can be explained by Fig. 6c and 6d, in which the length along  $y = 2$  becomes larger than that along  $y = 4$ , generating the spike on the half reaction surface. Nevertheless, the length along  $y = 2$  soon reaches its final position while the latter length along  $y = 4$  increases further, yielding the second intersection around  $t = 8.0$ . Moreover, these two curves show the slight overshoot of their steady positions. Although the overshoot is not significant, it deserves more attention for its potential impact on ODW applications. Formation of the intersection is due to the difference in the angle between the oblique shock and the oblique detonation. The oblique shock is generated by the wedge, while the oblique detonation is not only generated by the wedge but also supported by the post-shock heat release. It is observed that the oblique shock responses promptly when inflow parameters change, but the oblique detonation does not. Hence, the slow response of oblique detonation should be attributed to the effects of heat release, which induces the overshoot observed in Fig. 6 and previous studies [17].

### C. Upstream transition induced by increasing $\theta$

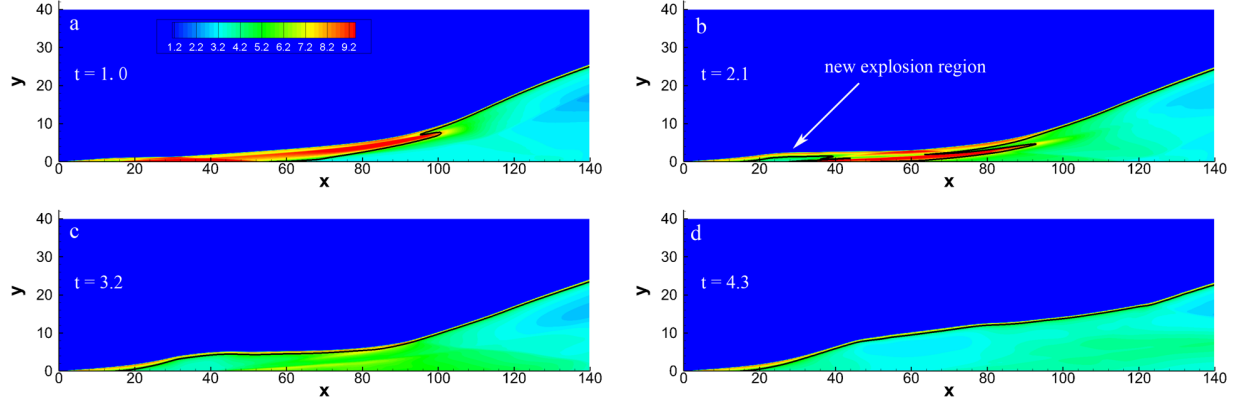


**Fig. 9 Evolution of the density field (with black line denoting  $\lambda = 0.5$ ) when  $\theta$  changes from  $18^\circ$  to  $24^\circ$ .**

By increasing  $\theta$  from  $18^\circ$  to  $24^\circ$ , the upstream dynamic transition is illustrated in Fig. 9, showing a different evolution process of the ODW initiation. Due to an increasing  $\theta$ , the post-oblique shock temperature and density rise accordingly, and Fig. 9a shows the high-density region close to the wedge tip. Subsequently, a new, isolated explosion region forms, denoted by the half reaction surface in Fig. 9b. At the same time, the initial reaction surface propagates upstream along the oblique wave, generating a corrugated reaction front into the premixed mixtures. The isolated explosion region soon combines with the upstream propagating reaction surface, generating a merged shock/reaction surface nearly parallel with the wedge, as shown in Fig. 9c. This merged structure featured by the parallel surface is unsteady and responds to the inflow by increasing the oblique detonation angle, as shown in Fig. 9d. The ODW structure eventually relaxes to be that shown in Fig. 3b.

To analyze the formation of the explosion region and related shock/reaction coupling, the evolution of the reaction progress  $\lambda$  on the wedge is shown in Fig. 10a. The initial black curve increases monotonically behind the oblique shock, but a  $\lambda$  peak forms around  $x = 12$  at the time instant  $t = 1.1$ , shown by the red curve (part of upstream curves is overlapped by the successive curves). Then the  $\lambda$  peak grows gradually, but its upstream part keeps the same, illustrated by the overlaid curves in Fig. 10. The curve trough rises slower than the curve crest, so the strength of  $\lambda$  peak increases in this period. Generally, the development of the upstream trough should be attributed to the explosion region, and the development of the downstream trough is linked to the original reaction region, which extends upstream due to the inflow variation. The new explosion region manifests during the time  $t = 0$  to 2.2, but the

propagation of the original reaction region dominates eventually between the time  $t = 2.2$  and  $5.5$ . Finally, the new explosion region and the original reaction front merge to establish the final ODW structure.

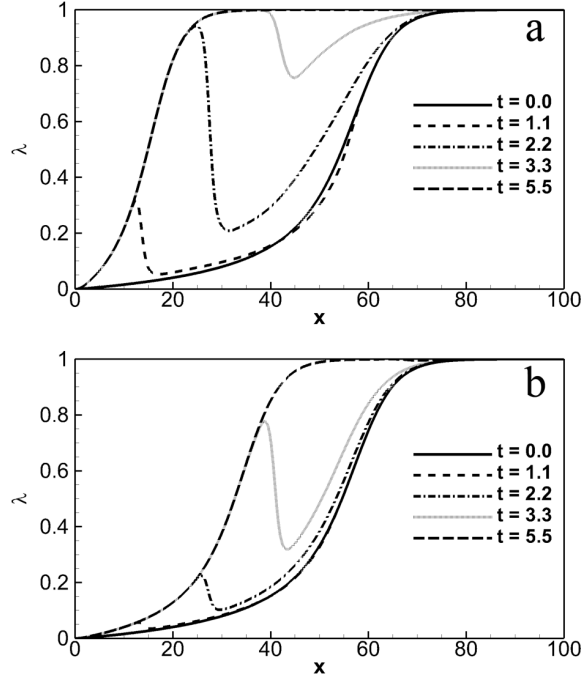


**Fig. 10** Reaction progress on the wedge when  $\theta$  changes from  $18^\circ$  to  $24^\circ$  (a) or  $20^\circ$  (b).

If the wedge angle increases from  $18^\circ$  to  $20^\circ$ , similar phenomena like Fig. 9 can be observed, featured by the formation of the new explosion region. Likewise, the new explosion region merges eventually with the original reaction surface, and the ODW structure relaxes gradually. The evolution of the reaction progress  $\lambda$  on the wedge when  $\theta$  changes from  $18^\circ$  to  $20^\circ$  is plotted in Fig. 10b. The new explosion region appears clearly, but its evolution is slower than the results shown in Fig. 10a. However, the evolution of the original reaction surface becomes much slower, which keeps almost the same from  $t = 0$  to  $3.3$ . Therefore, the new explosion region plays more important role in this structural transition, although it is weakened by the small angle increment.

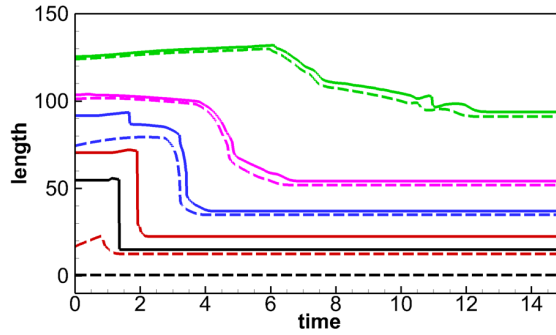


**Fig. 11** Initiation length (solid) and shock position (dashed) along  $y = 0$  (black), 1 (red), 5 (blue), 10 (pink), and 20 (green) when  $\theta$  changes from  $18^\circ$  to  $24^\circ$ .

The variation of the initiation length is shown in Fig. 11, with the oblique shock position also given by the dashed line. The step-like change in the initiation length can be observed clearly on the line  $y = 0$  and 1, but the shock position changes only on the line  $y = 1$ . This step-like change is originated from the growth of the discrete, new explosion region within the original oblique shock beginning from the wedge surface. On the lines  $y = 5, 10,$  and  $20$ , the effect of the new explosion region becomes progressively less prominent, but several turning points can still be observed clearly.

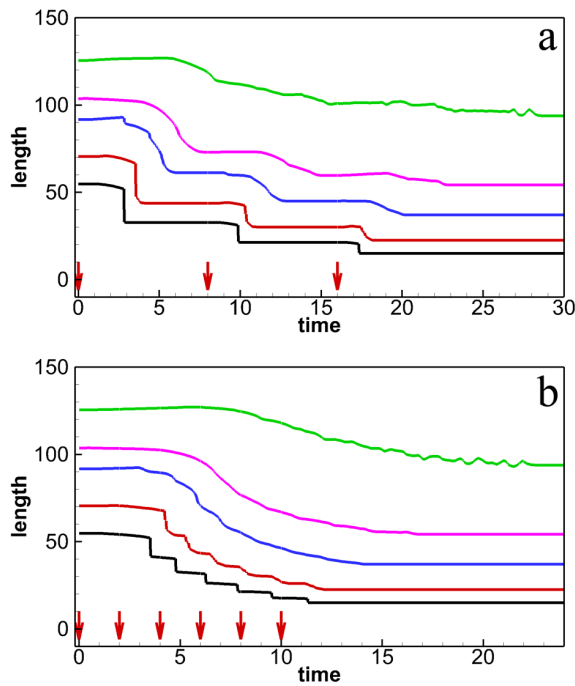


**Fig. 12** Initiation length along  $y = 0$  (black), 1 (red), 5 (blue), 10 (pink), and 20 (green) when  $\theta$  changes from  $18^\circ$  to  $24^\circ$ , (a) with the increment  $2^\circ$ ; (b) with the increment  $1^\circ$ .

The formation of the new explosion region only occurs in the upstream transition, which makes the transition complicated and may jeopardize the ODW application from a theoretical point of view. Because the effect of the new explosion region is shown to be weaker if the  $\theta$  variation is small, as shown in Fig. 10, a case study is performed by controlling the overall  $\theta$  variation in a quasi-static manner, i.e., to change  $\theta$  in incremental steps. The results from this idea are shown in Fig. 12a, with an incremental  $\theta$  change of  $2^\circ$  whose start time is denoted by the red arrow (the three red arrows denote that  $\theta$  changes into  $20^\circ$  at  $t = 0$ ,  $22^\circ$  at  $t = 8$ , and  $24^\circ$  at  $t = 16$ , respectively). These results illustrate a smoother change of the initiation length. In such cases, the step-wise behavior is minimized and the transition region moves upstream gradually towards the final equilibrium position. Meanwhile, the equilibrium oblique detonation in turn takes longer time, due to the long-time gradual angle variation, to establish as compared to the case with the angle change from  $18^\circ$  to  $24^\circ$  directly (see Fig. 10).

Further investigate on weakening the effects of new explosion region is performed by using smaller  $\theta$  increment and time interval. Generally, we found out that the upstream flow fields are easy to converge, but the downstream flow fields take a relatively long time. Considering the further  $\theta$  variation will change the downstream flow fields further, the convergence of the downstream flow fields is not necessary. Therefore, another case with an incremental angle change of  $1^\circ$  and a short time interval of 2 is simulated and the corresponding variation of the initial length is shown in Fig. 12b. It is observed that the variation with small angle change and short time interval induce a smoother transition process, and the step-like change in the initiation length becomes weak. Nevertheless, the relaxation process still requires a more significant time to complete than that of the case with  $\theta$  changing from  $18^\circ$  to  $24^\circ$  directly. The balance of the angle change and relaxation time thus needs to be taken into consideration in the actual ODW engine operation.

#### **IV. Concluding remarks**

In this study, the dynamics of the transition between two smooth ODW initiation structures with a curved shock induced by a semi-infinite wedge at high Mach number regime is investigated using numerical simulations. Specifically, this study aims to observe the unsteady evolution of the ODW structure and flow field in response to a wedge angle variation. By reducing the wedge angle, hence decreasing the strength of the oblique shock and reaction rate, the initiation position and transition process move downstream. The process is referred as “downstream



transition”. On the other hand, “upstream transition” is the process when the wedge angle increases (causing a higher post-oblique shock temperature accordingly) and the ODW formation occurs closer to the wedge-tip.

In the downstream transition, the change evolves around the original initiation point and the overall structure appears to move globally toward the final downstream location. Even though both the original and final stationary structures have the curved-shock configuration for the given flow conditions, a kink-like initiation structure, which is thought to be a more complicated structure, is observed intermediately during the transition process. Furthermore, different parts of the ODW structure reach their equilibrium positions at different time instants. The upstream part, mainly the oblique shock wave without local heat release, always converges first, and the downstream part takes longer time to converge.

In the upstream transition, an interesting distinct transition pattern appears which induces different wave dynamics. It is featured by a complex evolution with the formation of a new isolated reaction region, a corrugated reaction surface from the original initiation point, a transient coupled shock-reaction surface parallel to the wedge and its acceleration to establish the new structure corresponding to the new wedge angle. The formation of the new structure concerns two factors, one is the downstream extent of the new explosion region, and the other is the upstream extent of the original reaction surface. With a small angle variation, namely from  $18^\circ$  to  $20^\circ$ , the effects of the new explosion region become weak, but still dominate the initiation process. It is also observed that the upstream transition with an immediate angle change from  $18^\circ$  to  $24^\circ$  generates a step-like variation in the initiation length, mainly caused by the formation of the new reaction region. To minimize this step-like behavior, varying the wedge angle in a quasi-static manner over a finite relaxation time is suggested, and a smoother transition in term of the initiation length variation can be achieved.

These two transient processes demonstrate that the evolutions of the ODW flow fields are irreversible, and two different evolution paths are observed. From another view point, the wedge angle variation will make the OSW rebuilding first, and then a relatively slower response (convergence) of the combustion region. The transient processes induce the complicated phenomena, like the intermediate kink-like initiation structure, initiation length overshoot, new explosion region and so on, which is helpful in deepening knowledge on the flow in ODW engines. More fundamental studies on the transient process are thus necessary in the future.

## Acknowledgments

The research is supported by The National Natural Science Foundation of China NSFC No. 51376165, 11372333 and 91641130; and the Natural Sciences and Engineering Research Council of Canada (NSERC).

## References

- [1] Menees, G. P., Adelman, H. G., Cambier, J. and Bowles, J. V., “Wave combustors for trans-atmospheric vehicles”, *Journal of Propulsion and Power*, Vol. 8, No. 3, 1992, pp. 709–713.
- [2] Yi, T. H., Lu, F. K., Wilson, D. R., and Emanuel, G., “Numerical study of detonation wave propagation in a confined supersonic flow,” *Shock Waves*, Vol.27, No.3, 2017, pp. 395–408.
- [3] Fan, H. Y., and Lu, F. K., “Numerical modelling of oblique shock and detonation waves induced in a wedged channel,” *Proceedings of the Institute of Mechanical Engineers Part G – Journal of Aerospace Engineering*, 222(G5), 2008, pp. 687–703.  
doi: 10.1243/09544100JAERO273
- [4] Lu, F. K., Fan, H. Y., and Wilson, D. R., “Detonation waves induced by a confined wedge,” *Aerospace Science and Technology*, Vol. 10, No. 8, 2006, pp. 679–685.  
doi: 10.1016/j.ast.2006.06.005
- [5] Gross, R. A., “Oblique detonation waves,” *AIAA Journal*, Vol. 1, 1963, pp. 1225–1227.  
doi: 10.2514/3.1777
- [6] Pratt, D. T., Humphrey, J. W., and Glenn, D. E., “Morphology of standing oblique detonation waves,” *Journal of Propulsion and Power*, Vol. 7, No. 5, 1991, pp. 837–845.  
doi: 10.2514/3.23399
- [7] Ashford, S. A., and Emanuel, G., “Wave angle for oblique detonation waves,” *Shock Waves*, Vol. 3, No. 4, 1994, pp. 327–329.  
doi: 10.1007/BF01415831
- [8] Emanuel, G., and Tuckness, D. G., “Steady, Oblique, DetonationWaves,” *Shock Waves*, Vol. 13, No. 6, 2004, pp. 445–451.  
doi: 10.1007/s00193-003-0222-1c
- [9] Li, C., Kailasanath, K., and Oran, E. S., “Detonation structures behind oblique shocks,” *Physics of Fluids*, Vol. 6, No. 4, 1994, pp. 1600–1611.  
doi: 10.1063/1.868273

- [10] Li, C., Kailasanath, K. and Oran, E. S., "Effects of boundary layers on oblique-detonation structures," AIAA Paper 1993-0450.
- [11] Viguier, C., Figueira da Silva, L., Desbordes, D., and Deshaies, B., "Onset of oblique detonation waves: comparison between experimental and numerical results for hydrogen-air mixture," *Proceedings of the Combustion Institute*, Vol. 26, No. 2, 1996, pp. 3023–3031.  
doi: 10.1016/S0082-0784(96)80146-9
- [12] Figueira da Silva, L., and Deshaies, B., "Stabilization of an oblique detonation wave by a wedge: a parametric numerical study," *Combustion and Flame*, Vol. 121, 2000, pp. 152–166.  
doi: 10.1016/S0010-2180(99)00141-8
- [13] Papalexandris, M. V., "A numerical study of wedge-induced detonations," *Combustion and Flame*, Vol. 120, No. 4, 2000, pp. 526–538.  
doi: 10.1016/S0010-2180(99)00113-3
- [14] Teng, H. H., and Jiang, Z. L., "On the transition pattern of the oblique detonation structure," *Journal of Fluid Mechanics*, Vol. 713, 2012, pp. 659–669.  
doi: 10.1017/jfm.2012.478
- [15] Teng, H. H., Zhao, W., and Jiang, Z. L., "A novel oblique detonation structure and its stability," *Chinese Physics Letters*, Vol. 24, No. 7, 2007, pp. 1985–1988.  
doi: 10.1088/0256-307X/24/7/055
- [16] Choi, J. Y., Shin, E. J. R., and Jeung, I. S., "Unstable combustion induced by oblique shock waves at the non-attaching condition of the oblique detonation wave," *Proceedings of the Combustion Institute*, Vol. 32, No. 2, 2009, pp. 2387–2396.  
doi: 10.1016/j.proci.2008.06.212
- [17] Teng, H. H., Zhang, Y. N., and Jiang, Z. L., "Numerical investigation on the induction zone structure of the oblique detonation waves," *Computers and Fluids*, Vol. 95, 2014, pp. 127–131.  
doi: 10.1016/j.compfluid.2014.03.001
- [18] Liu, Y., Wu, D., Yao, S. B., and Wang, J. P., "Analytical and Numerical Investigations of Wedge-Induced Oblique Detonation Waves at Low Inflow Mach Number," *Combustion Science and Technology*, Vol. 187, No. 6, 2015, pp. 843–856.  
doi: 10.1080/00102202.2014.978865
- [19] Liu, Y., Liu, Y. S., Wu, D., and Wang, J. P., "Structure of an oblique detonation wave induced by a wedge," *Shock Waves*, Vol. 26, No. 2, 2016, pp. 161–168.  
doi: 10.1007/s00193-015-0600-5

- [20] Teng H. H., Ng, H. D., and Jiang, Z. L., "Initiation characteristics of wedge-induced oblique detonation wave in a stoichiometric hydrogen-air mixture," *Proceedings of the Combustion Institute*, Vol. 36, No. 2, 2017, pp. 2735–2742.  
doi: 10.1016/j.proci.2016.09.025
- [21] Grismer, M. J., and Powers, J. M., "Numerical predictions of oblique detonation stability boundaries," *Shock Waves*, Vol. 6, No. 3, 1996, pp. 147–156.  
doi: 10.1007/BF02510995
- [22] Choi, J. Y., Kim, D. W., Jeung, I. S., Ma, F., and Yang, V., "Cell-like structure of unstable oblique detonation wave from high-resolution numerical simulation," *Proceedings of the Combustion Institute*, Vol. 31, No. 2, 2007, pp. 2473–2480.  
doi: 10.1016/j.proci.2006.07.173
- [23] Verreault, J., Higgins, A. J., and Stowe, R. A., "Formation of transverse waves in oblique detonations," *Proceedings of the Combustion Institute*, Vol. 34, No. 2, 2013, pp. 1913–1920.  
doi: 10.1016/j.proci.2012.07.040
- [24] Teng, H. H., Jiang, Z. L., and Ng, H. D., "Numerical study on unstable surfaces of oblique detonations," *Journal of Fluid Mechanics*, Vol. 744, 2014, pp. 111–128.  
doi: 10.1017/jfm.2014.78
- [25] Teng, H. H., Ng, H. D., Li, K., Luo, C. T., and Jiang, Z. L., "Evolution of cellular structures on oblique detonation surfaces," *Combustion and Flame*, Vol. 162, No. 2, 2015, pp. 470–477.  
doi: 10.1016/j.combustflame.2014.07.021
- [26] Yang, P. F., Ng, H. D., Teng, H. H., and Jiang, Z. L., "Initiation structure of oblique detonation waves behind conical shocks," *Physics of Fluids*, Vol. 29, 2017, 086104  
doi: 10.1063/1.4999482
- [27] Cambier, J. L., Adelman, H., and Menees, G. P., "Numerical simulations of an oblique detonation wave engine," *Journal of Propulsion and Power*, Vol. 6, 1990, pp. 315–323.  
doi: 10.2514/3.25436
- [28] Vlasenko, V. V., and Sabel'nikov, V. A., "Numerical simulation of inviscid flows with hydrogen combustion behind shock waves and in detonation waves," *Combustion, Explosion, and Shock Waves*, Vol. 31, No. 3, 1995, pp. 376–389.  
doi: 10.1007/BF00742685
- [29] Iwata, K., Nakaya, S. and Tsue, M., "Wedge-stabilized oblique detonation in an inhomogeneous hydrogen-air mixture," *Proceedings of the Combustion Institute*. Vol. 36, No.2, 2017, pp. 2761–2769.  
doi: 10.1016/j.proci.2016.06.094

- [30] Zhang, Y. N., Gong, J. S., and Wang, T., “Numerical study on initiation of oblique detonations in hydrogen–air mixtures with various equivalence ratios,” *Aerospace Science and Technology*, Vol. 49, 2016, pp. 130–134.  
doi: 10.1016/j.ast.2015.11.035
- [31] Fusina, G., Sislian, J. P., and Parent, B., “Formation and stability of near Chapman-Jouguet oblique detonation waves,” *AIAA Journal*, Vol. 43, No. 7, 2005, pp. 1591–1604.  
doi: 10.2514/1.9128
- [32] Fang, Y. S., Hu, Z. M., Teng, H. H., Jiang, Z. L., and Ng, H. D., “Numerical study of inflow equivalence ratio inhomogeneity on oblique detonation formation in hydrogen-air mixtures,” *Aerospace Science and Technology*, Vol 71, 2017, pp. 256–263.  
doi: 10.1016/j.ast.2017.09.027
- [33] Dubebout, R., Sislian, J. P., and Oppitz, R., “Numerical simulation of hypersonic shock-induced combustion ramjets,” *Journal of Propulsion and Power*, Vol. 14, No. 6, 1998, pp. 869–879.  
doi: 10.2514/2.5368
- [34] Toro, E. F., *Riemann solvers and numerical methods for fluid dynamics*, 2<sup>nd</sup> ed., Springer, Berlin, 1999.
- [35] Ng, H. D., Higgins, A., Kiyanda, C., Radulescu, M., Lee, J. H., Bates, K., and Nikiforakis, N., “Nonlinear dynamics and chaos analysis of one-dimensional pulsating detonations,” *Combustion Theory and Modelling*, Vol. 9, 2005, pp. 159–170.  
doi: 10.1080/13647830500098357
- [36] Henrick, A. K., Aslam, T. D., and Powers, J. M., “Simulations of pulsating one-dimensional detonations with true fifth order accuracy,” *Journal of Computational Physics*, Vol. 213, 2006, pp. 311–329.  
doi: 10.1016/j.jcp.2005.08.013
- [37] Gamezo, V. N., Desbordes, D., and Oran, E. S., “Two-dimensional reactive flow dynamics in cellular detonation waves,” *Shock Waves*, Vol. 9, 1999, pp. 11–17.  
doi: 10.1007/s001930050134
- [38] Gamezo, V. N., Desbordes, D., and Oran, E. S., “Formation and evolution of two-dimensional cellular detonations,” *Combustion and Flame*, Vol. 116, 1999, pp. 154–165.  
doi: 10.1016/S0010-2180(98)00031-5
- [39] Sharpe, G. J., “Linear stability of pathological detonations,” *Journal of Fluid Mechanics*, Vol. 401, 1999, pp. 311–338.  
doi: 10.1017/S0022112099006655
- [40] Sharpe, G. J., and Falle, S.A.E.G., “One-dimensional nonlinear stability of pathological detonations,” *Journal of Fluid Mechanics*, Vol. 414, 2000, pp. 339–366.  
doi: 10.1017/S0022112000008697

[41] Wang, T., Zhang, Y. N., Teng, H. H., Jiang, Z. L., and Ng, H. D., “Numerical study of oblique detonation wave initiation in a stoichiometric H<sub>2</sub>-air mixture,” *Physics of Fluids*, Vol. 27, 2015, 096101.

doi: 10.1063/1.4930986

[42] Mazaheri, K., Mahmoudi, Y., and Radulescu, M. I., “Diffusion and hydrodynamic instabilities in gaseous detonations,” *Combustion and Flame* Vol. 159, 2012, pp. 2138–2154.

doi: 10.1016/j.combustflame.2012.01.024